Magneto-optical effects in interacting localized and propagating surface plasmon modes

Jorge F. Torrado, Juan B. González-Díaz, María U. González, Antonio García-Martín, and Gaspar Armelles*

IMM-Instituto de Microelectrónica de Madrid (CNM-CSIC), Isaac Newton 8, PTM,
E-28760 Tres Cantos, Madrid, Spain
*gaspar.armelles@imm.cnm.csic.es

Abstract: We report that the effect of an external magnetic field on the propagation of surface plasmons can be effectively modified through the coupling between localized (LSP) and propagating (SPP) surface plasmons. When these plasmon modes do not interact, the main effect of the magnetic field is a modification of the wavevector of the SPP mode, leaving the LSP virtually unaffected. Once both modes start to interact, there is a strong variation of the magnetic field induced modification of the SPP dispersion curve and, simultaneously, the LSP mode becomes sensitive to the magnetic field.

References and links

1. V. A. Fedotov, P. L. Mladyonov, S. L. Prosvirnin, A. V. Rogacheva, Y. Chen, and N. I. Zheludev, "Asymmetric propagation of electromagnetic waves through a planar chiral structure," Phys. Rev. Lett. **97**(16), 167401 (2006).
2. A. Zvezdin, and V. Kotov, *Modern Magnetooptics and Magnetooptical Materials*, Condensed Matter Physics (Taylor and Francis Group, New York, 1997).
3. A. Figotin, and I. Vitebskiy, "Electromagnetic unidirectionality in magnetic photonic crystals," Phys. Rev. B **67**(16), 165210 (2003).
4. Z. Yu, Z. Wang, and S. Fan, "One-way total reflection with one-dimensional magneto-optical photonic crystals," Appl. Phys. Lett. **90**(12), 121133 (2007).
5. F. D. M. Haldane, and S. Raghu, "Possible realization of directional optical waveguides in photonic crystals with broken time-reversal symmetry," Phys. Rev. Lett. **100**(1), 013904 (2008).
6. Z. Wang, Y. D. Chong, J. D. Joannopoulos, and M. Soljačić, "Reflection-free one-way edge modes in a gyromagnetic photonic crystal," Phys. Rev. Lett. **100**(1), 013905 (2008).
7. Z. Yu, G. Veronis, Z. Wang, and S. Fan, "One-way electromagnetic waveguide formed at the interface between a plasmonic metal under a static magnetic field and a photonic crystal," Phys. Rev. Lett. **100**(2), 023902 (2008).
8. Z. Wang, Y. Chong, J. D. Joannopoulos, and M. Soljačić, "Observation of unidirectional backscattering-immune topological electromagnetic states," Nature **461**(7265), 772–775 (2009).
9. W. L. Barnes, A. Dereux, and T. W. Ebbesen, "Surface plasmon subwavelength optics," Nature **424**(6950), 824–830 (2003).
10. E. Ozbay, "Plasmonics: merging photonics and electronics at nanoscale dimensions," Science **311**(5758), 189–193 (2006).
11. V. V. Temnov, G. Armelles, U. Woggon, D. Guzatov, A. Cebollada, A. García-Martín, J. García-Martín, T. Thomay, A. Leitenstorfer, and R. Braschitsch, "Active magnetoplasmonics in hybrid metal/ferromagnet/metal microinterferometers," Nat. Photonics **4**, 107 (2010).
12. R. F. Wallis, in *Electromagnetic surface modes* (John Wiley & Sons, 1982), chap. 15 – Surface magnetoplasmons on semiconductors, pp. 575–631.
13. R. E. Camley, "Nonreciprocal surface waves," Surf. Sci. Rep. **7**(3-4), 103–187 (1987).
14. S. C. Kitson, W. L. Barnes, and J. R. Sambles, "Full Photonic Band Gap for Surface Modes in the Visible," Phys. Rev. Lett. **77**(13), 2670–2673 (1996).
15. C. Hermann, V. A. Kosobukin, G. Lampel, J. Peretti, V. I. Safarov, and P. Bertrand, "Surface-enhanced magneto-optics in metallic multilayer films," Phys. Rev. B **64**(23), 235422 (2001).
16. J. B. González-Díaz, A. García-Martín, G. Armelles, J. M. García-Martín, C. Clavero, A. Cebollada, R. A. Lukascew, J. R. Skuza, D. P. Kumah, and R. Clarke, "Surface-magnetoplasmon nonreciprocity effects in noble-metal/ferromagnetic heterostructures," Phys. Rev. B **76**(15), 153402 (2007).

17. E. Ferreiro-Vila, J. B. González-Díaz, R. Fermento, M. U. González, A. García-Martín, J. M. García-Martín, A. Cebollada, G. Armelles, D. Meneses-Rodríguez, and E. Muñoz-Sandoval, "Intertwined magneto-optical and plasmonic effects in Ag/Co/Ag layered structures," Phys. Rev. B **80**(12), 125132 (2009).
18. J. Cesario, R. Quidant, G. Badenes, and S. Enoch, "Electromagnetic coupling between a metal nanoparticle grating and a metallic surface," Opt. Lett. **30**(24), 3404–3406 (2005).
19. A. Christ, T. Zentgraf, S. G. Tikhodeev, N. A. Gippius, J. Kuhl, and H. Giessen, "Controlling the interaction between localized and delocalized surface plasmon modes: Experiment and numerical calculations," Phys. Rev. B **74**(15), 155435 (2006).
20. T. A. Kelf, Y. Sugawara, J. J. Baumberg, M. Abdelsalam, and P. N. Bartlett, "Plasmonic band gaps and trapped plasmons on nanostructured metal surfaces," Phys. Rev. Lett. **95**(11), 116802 (2005).
21. Y. Chu, and K. B. Crozier, "Experimental study of the interaction between localized and propagating surface plasmons," Opt. Lett. **34**(3), 244–246 (2009).
22. A. Ghoshal, I. Divliansky, and P. G. Kik, "Experimental observation of mode-selective anticrossing in surface-plasmon-coupled metal nanoparticle arrays," Appl. Phys. Lett. **94**(17), 171108 (2009).
23. C. Dehesa-Martinez, L. Blanco-Gutierrez, M. Vélez, J. Diaz, L. M. Alvarez-Prado, and J. M. Alameda, "Magneto-optical transverse Kerr effect in multilayers," Phys. Rev. B **64**(2), 024417 (2001).
24. G. Armelles, J. B. González-Díaz, A. García-Martín, J. M. García-Martín, A. Cebollada, M. Ujué González, S. Acimovic, J. Cesario, R. Quidant, and G. Badenes, "Localized surface plasmon resonance effects on the magneto-optical activity of continuous Au/Co/Au trilayers," Opt. Express **16**(20), 16104–16112 (2008), http://www.opticsexpress.org/abstract.cfm?URI=oe-16-20-16104.
25. J. B. González-Díaz, A. García-Martín, J. M. García-Martín, A. Cebollada, G. Armelles, B. Sepúlveda, Y. Alaverdyan, and M. Käll, "Plasmonic Au/Co/Au nanosandwiches with enhanced magneto-optical activity," Small **4**(2), 202–205 (2008).
26. A. García-Martín, G. Armelles, and S. Pereira, "Light transport in photonic crystals composed of magneto-optically active materials," Phys. Rev. B **71**(20), 205116 (2005).

1. Introduction

Optical systems providing asymmetric propagation between the backward and forward directions are interesting both from the fundamental and the applied point of view [1]. This property is well known in magneto-optical materials [2], and for example in conventional optics the design of most optical isolators relies on the Faraday effect. The structuration of the magneto-optical dielectrics in what are called magnetic photonic crystals allows a further control of the effect of the magnetic field on the propagation of light, and with an appropriate design the magnetic field induced modification of the photonic band structure could be as important as to allow the appearance of unidirectional propagating modes [3–8]. These works have opened the door to a new range of magneto-photonic devices immune to back-scattering losses. Considering that surface plasmons (SP) are a promising route toward the development of miniaturized photonic devices [9,10], and that the magneto-optical actuation in magneto-plasmonic microinterferometers has already been demonstrated [11], it seems appropriate to analyze the effect of the nanostructuration of plasmonic system on their behavior under an applied magnetic field.

In a flat and non-structured metal-dielectric interface, a magnetic field applied in the plane of the interface and perpendicular to the SP propagation direction adds a linear modification to the SP wavevector [7,11–13], leading to an asymmetric propagation of the SP in the forward and backward direction ($\omega(k) \neq \omega(-k)$). If the interface is nanostructurated, the dispersion relation of the surface plasmon is modified [14] and this could change the effect that the applied magnetic field has on the surface plasmon propagation. In this letter, we examine the variation under an applied magnetic field of the SP band structure of a metallic plasmonic crystal consisting on a magnetoplasmonic layer, a dielectric spacer and an array of Au nanodisks deposited on the top. Magnetoplasmonic layers are hybrid structures made of noble and ferromagnetic metals, so that its magneto-optical activity is governed by the ferromagnetic component and appreciable changes of the optical properties can be obtained by applying low magnetic fields [11,15–17]. Our metallic plasmonic crystal sustains two kinds of SP modes: localized (LSP) on the Au nanodisks and propagating or surface plasmon polaritons (SPP) on the magnetoplasmonic layer, as in purely plasmonic systems [18,19]. Upon the right excitation conditions these two plasmon modes may interact [19–22], modifying the dispersion curves and leading to hybrid LSP/SPP modes due to the strong

coupling between them. Here we show that, through the analysis of the magneto-optical response, we are able to follow this interaction/hybridization process. Moreover, we demonstrate that these interactions substantially alter the effect of the magnetic field on both SP modes. This result points out the feasibility of designing more complex magnetoplasmonic structures with tailored asymmetric propagation.

2. Magneto-optical measurements configuration

Samples were fabricated using several deposition and lithography steps. A trilayer of 16 nm Au / 10 nm Co/ 6 nm Au was deposited on glass by sputtering and covered by a thermally evaporated 20 nm thick SiO_2 layer. Squared arrays of gold nanodisks were fabricated on top by means of electron beam lithography followed by thermal evaporation and lift-off. The disk diameter and height are 110 nm and 20 nm respectively. The array period has been varied from 300 nm to 400 nm.

The sketch of the experimental configuration is displayed as an inset in Fig. 1. The magnetic field is applied in the plane of the sample (xy) and perpendicular to the plane of incidence (xz). The incident and reflected light are p-polarized. The lower inset on the figures shows the dependence of the reflected light (measured at wavelength 532 nm) on the applied magnetic field. This provides information on the magnetic field dependence of the y component of the Co layer magnetization M_y. The shape of this loop is the same in sample regions with and without disks. As can be seen, the magnetic field needed to saturate the Co layer is 10 mT. The transverse Magneto-Optical Kerr Effect (TMOKE) signal is then defined as the normalized difference of the reflectivity upon reversal at saturation:

$$TMOKE \equiv \frac{R(+M) - R(-M)}{R(+M) + R(-M)}. \tag{1}$$

Figure 1(a) shows the TMOKE signal for an angle of incidence θ_{inc} of 50 degrees and a period of the array of 300 nm, together with that of one sample region without disks (consisting only of the metallic trilayer covered by the SiO_2 layer). As can be observed, the TMOKE signal of the region without disks shows no particular features and its intensity decreases as we increase the wavelength, as expected for MO response of a continuous Co film [23]. On the other, the spectrum of the disks region presents additional features that can be associated with the LSP and SPP modes as we will see below. At this point, we would like to point out that the TMOKE allows to distinguish the SPP from the LSP. For the SPP the magnetic field modulates the SPP wavevector, which induces a shift of the reflectivity curve [16,17], manifesting thus in a "S-type" shape signal, whereas for the LSP the effect is a variation of the intensity [24,25], giving rise to a "peak-type" signal.

To unmask the TMOKE signal from the featureless spectral shape associated with the MO response of the continuous Co layer, we will analyze the difference between the TMOKE signal of the regions with and without disks. This "renormalized" TMOKE is seen in Fig. 1(b) where the two structures, S-like and peak-type, labeled P1 (Δ) and L (O) respectively, are depicted and their energy locations are to be taken at the zero-crossing of the S-feature for P1 and at the top most of the peak for L.
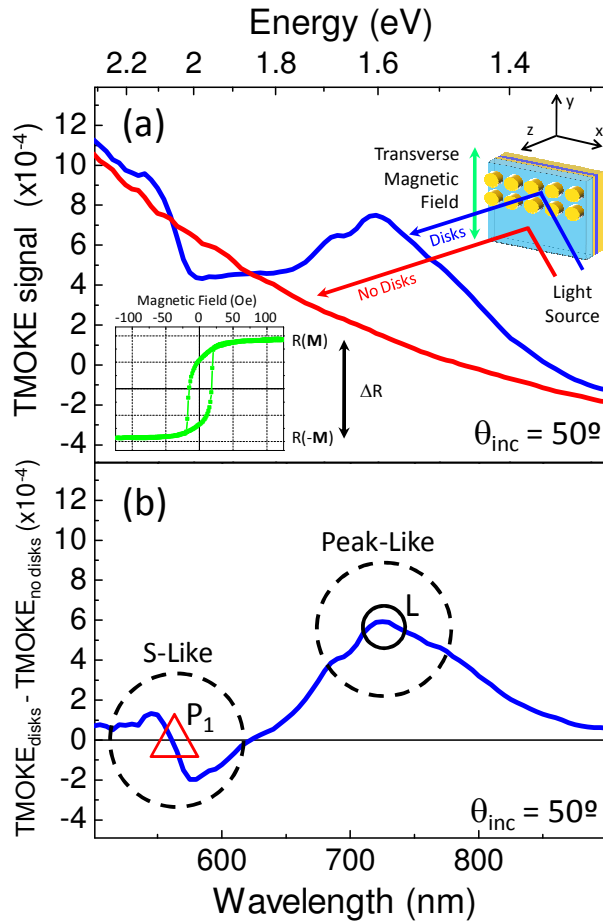
Fig. 1. (a) Spectral dependence of the TMOKE signal for an angle of incidence of 50° in the regions without and with (300 nm array periodicity) gold disks. The insets show the sketch of the experimental configuration and the evolution of the reflectivity with the applied magnetic field. (b) "Renormalized" TMOKE signal, corresponding to the TMOKE signal of the region with disks minus that of the region without disks.

3. Results and discussion

Figure 2 shows the TMOKE signal as a function of the incident angle for two different array periods. The spectra are shifted for clarity. As can be observed, the spectral location of P1 depends on both the incident angle and array period whereas that of L is basically independent of those parameters. This reinforces our previous statement, allowing us to associate the structure L with the LSP of gold disks and P1 with a SPP of the trilayer. Since it is the periodic disks array which enables the coupling of light with the propagating surface plasmon modes of the trilayer, the energy at which the in-plane wavevector of the incident light matches the SPP wavevector will depend on both the incident angle and the array period [18–20]. The position of the P1 structure is consistent with the SPP mode localized at the trilayer / 20 nm SiO_2 interface (upper SPP mode), which has a higher frequency than that of the SPP mode located at the trilayer / glass substrate interface (lower SPP mode). It is worth noticing that we have hints in the TMOKE spectra of a second S-like structure at lower frequencies corresponding to this lower SPP mode, but it is too weak to unambiguously discern it within the noise level (below 1×10^{-4}).

When analyzing the position of feature L in more detail, it can be seen that when P1 gets near its energy position experiments a small shift. This indicates that the SPP responsible for P1 interacts with the LSP associated with L when the spectral separation of the two plasmon modes is small [19–22]. The bottom graphs of Fig. 2 show the spectral evolution of the two features and their interaction, with the anticrossing behavior characteristic of strong coupling between LSP and SPP, similar to that observed in previous works [19–22]. The dashed lines are guides for the eyes.
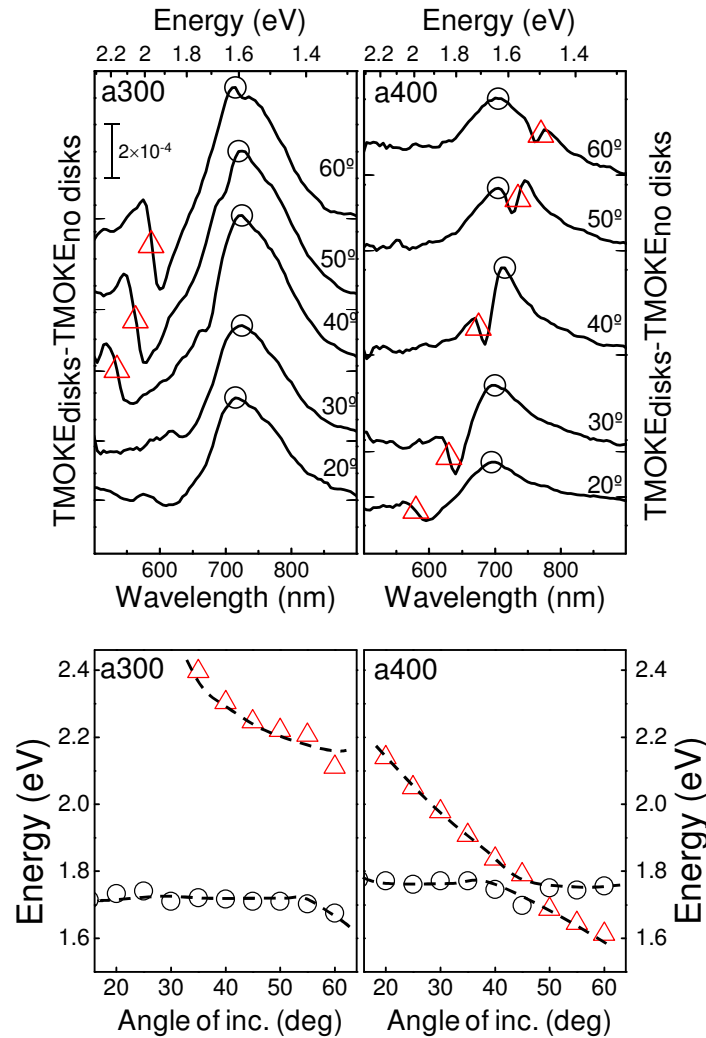

Fig. 2. Evolution with the angle of incidence of the TMOKE spectra for arrays of periodicity 300 nm (upper left) and 400 nm (upper right). The spectra are shifted for clarity, and the small marks in the lateral axes indicate the zero level for each curve. The bar in the upper left side of the left graph shows the graphs scale. The bottom graphs show the evolution with the angle of incidence of the two different features observed in the spectra: propagating surface plasmon (P1, Δ) and localized surface plasmon (L, O). The dashed lines are guides for the eyes pointing out the anticrossing behavior at the interaction region.

Let us now analyze in detail the two main features P1 and L appearing in the TMOKE spectra. Figure 3(a) shows a schema of the folded dispersion curve of the upper SPP mode of the trilayer for two different orientations of the magnetization in the Co layer: for a fixed

angle of incidence, the frequency at which the in-plane wavevector of the incident light matches that of the SPP depends on the orientation of the Co layer magnetization. Since the effect is small, in a first order approximation the change in the reflectivity induced by the switching of the Co magnetization (TMOKE signal) should be similar to the derivative of the reflectivity with respect to energy:

$$R(+M) - R(-M) \simeq \frac{\partial R}{\partial E} \Delta E, \tag{2}$$

where ΔE is a proportionality factor that accounts for the magnitude of the magnetic field-induced SPP wavevector modulation. Figure 3(b) presents both the TMOKE spectra and the energy derivatives of the reflectivity for the sample with 400 nm period disks array and for the angles of incidence of 20, 30 and 40 degrees. As can be observed, in the spectral region of the propagating mode P1 the two curves have a similar shape, which confirms that for propagating surface plasmons modes the main effect of applying a magnetic field is indeed to modify the SPP wavevector. On the other hand, in the region of the LSP mode the two curves are different, indicating that the magnetic field does not modify the frequency of this localized mode. In the case of the LSP, the presence of the Au disks arrays produces a minimum in the reflectivity at the spectral position of the LSP, giving rise to the aforementioned peak shape in the TMOKE spectra, signaling to a mainly optical origin and not related to magnetic modulation.
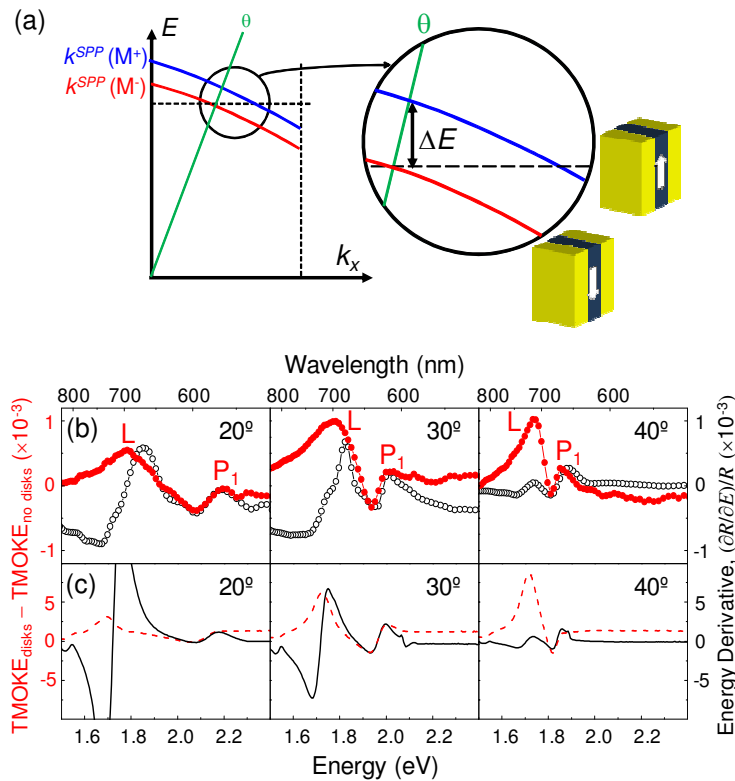

Fig. 3. (a) Schema of the modification of the SPP dispersion relation under switching of the Co layer magnetization. (b) Experimental TMOKE spectra (closed symbols) for the sample with a disks array of period 400 nm for three different angles of incidence, together with the energy derivatives of the reflectivity (open symbols). (c) Calculated TMOKE spectra (dashed lines) and energy derivatives of the simulated reflectivity (continuous lines) for the same system.

From a comparison of the intensity of the P1 feature of the TMOKE spectra and the same feature in the energy derivative spectra (see Eq. (2), we can extract the magnitude of the SPP wavevector modulation, ΔE, for different SPP frequencies. ΔE represents indeed the degree of propagation asymmetry, and the results are presented in Fig. 4(b) with red triangles. As can be observed, for the smallest wavevectors ΔE has a nearly constant value, and it starts to decrease at higher wavevectors, those at which the LSP and SPP modes start to interact (see Fig. 2 or Fig. 4(a)). This suggests that this behavior is related to the interaction of the localized and propagating modes of the structure.

To get a deeper insight on this interaction effect, we have performed a calculation based on scattering matrix formalism with magnetooptics included [26], using the materials optical and magnetooptical constant experimentally determined [17]. We can both simulate the spectra and calculate the frequency of the different plasmon modes for different orientation of the Co magnetization. As an example, we present in Fig. 3 the calculated TMOKE spectra (dashed lines) and the calculated energy derivative spectra of the reflectivity (continuous line) for the same configuration as in the experimental data. As can be observed the theoretical spectra follow the same trends as the experimental ones: features associated with the propagating and localized modes appear, and they start to interact when this frequencies approach. The calculated dispersion relations of the two modes are shown in Fig. 4(a).
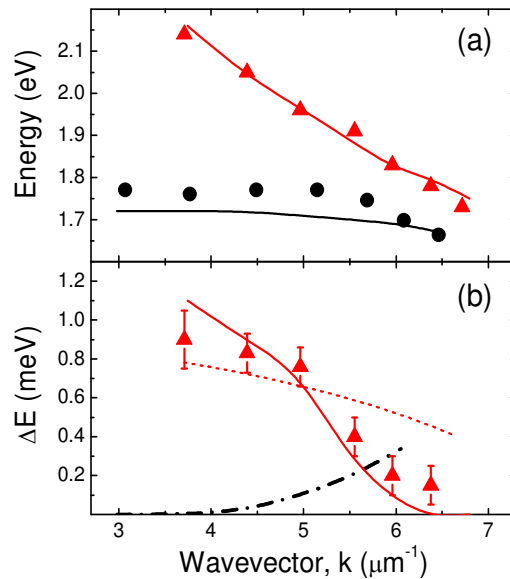

Fig. 4. (a) Experimental dispersion relations of the LSP and SPP modes for the sample with an array of period 400 nm, extracted from the TMOKE spectra shown in Fig. 2 (solid symbols), together with the dispersion relation extracted from calculations (continuous lines). (b) Evolution of the magnetic field-induced modulation for the different plasmon modes: LSP (dot-dashed black line, theory), SPP (red continuous line for theory, triangles for experimental data) and SPP for a $SiO_2/Au/Co/Au$ multilayer system without disks array on top (dotted red line, theory).

Moreover, the theoretical spectra shown in Fig. 3 also confirm that the main effect of the magnetic field on the SPP is to modify its wavevector, since in the spectral region of the SPP mode the theoretical TMOKE spectra and the energy derivative spectra have a similar shape. The calculated magnetic field-induced modification of the SPP wavevector, ΔE, is also shown in Fig. 4(b) (continuous red line). As can be observed the theoretical curve reproduces the experimental trends: as we increase the k value the modification of the SPP wavevector decreases. On the other hand, the calculated spectra also allows to extract the ΔE

modifications for the LSP (dot-dashed black line), which experimentally are beyond the resolution capabilities of our system. For the LSP, ΔE increases as we increase the k value, and this increase is due to the interaction with the SPP mode. In the interaction region there is a transfer of character between the localized and the propagating modes, and in particular we see here how the magnetic field-induced effect decreases in the SPP mode to pass to the LSP one. We understand this exchange of sensitivity to the magnetic field between the two plasmon modes as a direct demonstration of the strong coupling between them. Finally, the dotted line included in Fig. 4(b) corresponds to the calculated SPP wavevector modulation for a Au/Co/Au trilayer covered by 20 nm SiO_2 with no disks on the top, showing as a reference the values of the modulation when no LSP-SPP interaction is involved (note that the k values here have been translated by one reciprocal wavevector to plot this modulation together with the values corresponding to the metallic plasmonic crystal structure). As can be seen, there is a small dependence of ΔE with the wavevector, due to the spectral behavior of the magneto-optical constants; however, this dependence is much less abrupt than in the case comprising LSP-SPP interaction.

4. Conclusions

Summarizing, far from the LSP-SPP interaction region, the magnetic field induces the expected wavevector modification for the SPP mode whereas the frequency of the LSP mode hardly depends on the Co magnetization. However, once both modes start to interact and due to their coupling, there is a strong reduction of the dependence of the SPP dispersion curve with the Co magnetization, this dependence being transferred to the LSP mode. Moreover, in this work we have analyzed the situation with a fixed thickness of the SiO_2 spacer layer. Being the surface plasmons surface waves with exponential decays, the interaction between both modes will be highly dependent on the thickness of the spacer and the overlap between the two modes. The analysis of the behavior of the system as a function of the thickness of the SiO_2 layer would be of high interest, in order to identify the configuration of maximum coupling between the two modes.

From a more general point of view, these results show that the nanostructuration of the magnetoplasmonic system does indeed modify the effect of the magnetic field on the SP modes, being this study a first step towards the development of more complex systems where the asymmetric propagation of surface plasmons can be further engineered.

Acknowledgments